A 2.4-GHz CMOS Short-Range Wireless-Sensor-Network Interface for Automotive Applications

João Paulo Carmo, *Member, IEEE*, Paulo Mateus Mendes, *Member, IEEE*, Carlos Couto, *Senior Member, IEEE*, and José Higino Correia, *Member, IEEE*

***Abstract*—This paper describes a CMOS interface for short-range wireless sensor networks (CMOS-SRWSN interface). The sensor interface is composed of a sensor readout, electronics for processing and control, a memory, a radio-frequency CMOS transceiver for operation in the 2.4-GHz industrial, scientific, and medical bands, and a planar antenna. The receiver has a sensitivity of −60 dBm and consumes 6.3 mW from a 1.8-V supply. The transmitter delivers an output power of 0 dBm with a power consumption of 11.2 mW. The application of the CMOS-SRWSN interface is in the automotive industry for the reduction of cables and to support the information, communication, and entertainment systems in cars.**

***Index Terms*—Automotive sensors, sensor interface, wireless microsystems, wireless sensor networks.**

I. Introduction

SENSORS have been applied in automobiles, ever since the introduction of the manifold air pressure sensor for engine control in 1979, followed by airbag sensors in the mid-1980s. Furthermore, microsystems have been increasingly used throughout the vehicle. The demand of new sensing and management applications undoubtedly leads to more intelligent cars and the increased need of a networking infrastructure to connect the whole range of sensors and actuators. The system environment of an automobile is becoming more and more complex. While, formerly, one single supplier delivered all components of an antilock braking system or all sensors for airbag control, today, the networked architecture allows merged sensor systems for different functions. Ambient intelligence, which means an environment of interacting smart devices, is opening up new information sources for the vehicle. With the growing use of bus systems, building exclusive systems for each function is becoming more and more difficult and too expensive [1]. A present-day wiring harness may have up to 4000 parts, weigh as much as 40 kg, and contain more than 1900 wires for up to 4 km of wiring [2]. Thus, these networks bring serious drawbacks like reliability, maintenance, and constraints if the manufacturer plans the addition of new functions. These drawbacks can be avoided with wireless transmission infrastructures. Using multichip-module (MCM) techniques, it is possible to assemble, in the same microsystem, the sensors, a radio-frequency (RF) transceiver, electronics of processing and control, a memory, and an associated antenna [3]. In the last years, the potential to use wireless interfaces in the vehicular industry became an important goal [2], [4]–[13]. In this context, this paper presents a complete wireless interface (the CMOS short-range wireless-sensor-network (CMOS-SRWSN) interface) for use in cars. The CMOS-SRWSN interface is composed of an RF transceiver, an integrated antenna, and electronics of control and processing for connecting to sensors with analog and digital outputs.

Manuscript received August 5, 2008; revised August 24, 2009. First published September 22, 2009; current version published April 14, 2010.

The authors are with the Department of Industrial Electronics, University of Minho, 4800-058 Guimarães, Portugal (e-mail: jcarmo@dei.uminho.pt; pmendes@dei.uminho.pt; ccouto@dei.uminho.pt; higino.correia@dei.uminho.pt).

Color versions of one or more of the figures in this paper are available online at http://ieeexplore.ieee.org.

Digital Object Identifier 10.1109/TIE.2009.2032207

II. Current State-of-the-Art and System Overview

Advances made in the electronics industry in general and government legislation toward the increase of comfort and safety in cars were the main driving forces that led to the development of vehicle network technologies. Recently, the autoradio was considered the only electronic device in a vehicle, but now, almost every existing component in the vehicle has some sort of electronic feature. Electronic modules are placed in the automobile in order to acquire the measures of the sensors (speed, temperature, and pressure, among others) and to be used in computations. The orders received by the various actuators are given by these same modules, which are responsible for actions, where the switching on the cooling fan and changing gear (in the case of automatic gears) constitute some examples of actuation. These modules must exchange data between each other during the normal operation of the vehicle. An example of such data exchange is when a communication between the engine and the transmission of a car is needed in order to exchange information with other modules when a gear shift occurs. This need of a fast and reliable data exchange leads to the development of the vehicle network concept. Moreover, the use of microcomputers, electronic display, and voice output in motor vehicles means greater scope not only for the gathering and processing data but also for making such data available to the driver [14].

There are several network types and protocols used in vehicles by various manufacturers, but the controller area network (CAN), which is an inexpensive low-speed serial bus for interconnecting automotive components, is the most used by

the vehicular industry [15]. CAN has been running in cars for more than ten years now. However, unlike the telecom industry, which has managed to establish a Global System for Mobile communications standard where every service provider can use components from the worldwide supplier ecosystem, the car industry has not moved beyond a component standard for CAN.

The General Motors Company was the first, if not the only one up to now, to have the idea to install wireless links in vehicles, in order to replace cables [2]. Mainly, these cables are based on low-current loops that simultaneously feed and acquire data from the sensors. However, the specificity of the environment in a car addresses aspects that are not present in other types of wireless networks. Thus, a wireless network to connect sensors in a car is not just another type of wireless sensor network. Previous studies conducted in a vehicular environment revealed a set of issues, which cannot be discarded [2], [4]. The most important aspect to be considered is the question of heterogeneity, where different sensors and different communication profiles are present and must coexist [4]. The characterization of the wireless channel and the choice of the most suitable modulation are other important and definitive aspects [5]–[10]. In terms of reliability, the work presented in [5] for the frequency of 915 MHz with BPSK modulation and using a forward-error-correction code showed a network support of at least 98% packet reception rate. Moreover, it is also suggested that, with a sacrifice in the throughput, an automatic repeat request (ARQ) scheme will result in a better packet reception. Furthermore, further works suggested that using ultrawideband transmission makes it possible to achieve high data rates, despite the noisy and fading characteristics of the in-CAN environment [6]–[8].

In spite of an extensive number of studies relative to the characterization of radio channels inside vehicles, it is an evident effort to try to put the vehicular sensors, controllers, and multimedia systems in connection using emerging and established technologies, such as ZigBee [2], [4], [10] and Bluetooth [11]–[13]. These two standards have their strong points and drawbacks. ZigBee is a set of protocols (e.g., corresponding to the two lowest layers in the Open System Interconnection model) that allows one to mount a real wireless sensor network in topologies ranging from a simple star to complex meshes with the advantage to work for years. This working mode is obtained at a cost to have the wireless nodes to operate in low duty cycles. Low duty cycles are not tolerable in real-time systems; therefore, the advantage of ZigBee will quickly turn into something to avoid. Alternatively, Bluetooth allows the use of high baud rates, e.g., baud rates up to 1 Mb/s, to exchange data between the wireless nodes. However, it is very difficult to have complex mesh topologies, and worse, Bluetooth is a very heavy protocol with a lot of rules, where, despite the high baud rates available, it will result in high latencies. High latencies are also unacceptable in real-time monitoring and control systems. Thus, Bluetooth is more suitable in applications such as hand-free systems that allow drivers to keep their hands on the wheel while staying connected to cellular phones. Furthermore, the use of a high density of nodes and simple protocols in the vehicular environment was also tried before [9], [16]. Several variants for the same solution were proposed, and all of the implementations used third-party products such as radios (motes) and sensor interfaces [16]. These motes are ready-to-use wireless modules, where boards with sensors are attached. Their primary advantage rapidly fades and turns into a severe drawback, because the primary goal is to have wireless platforms integrating the vehicular environment. Thus, more compact and low-sized modules are needed. Furthermore, these solutions are much too expensive for high mass production and, thus, for use in cars.

The advantages of having RF transceivers with dimensions comparable to the other elements of the microsystem, such as the sensors and the electronics of processing and control, are enormous. Miniaturized microsystems contribute to the mass production with low prices, favoring the spread of applications for these microsystems. Moreover, solutions relying in wireless microsystems, offer a flexibility such that it is possible to choose how many and which sensors are to be integrated together with the RF transceiver and remaining electronics. The CMOS-SRWSN interface has low-power and low-voltage features. Furthermore, it can control the power during the transmission and select what subsystem must be enabled. The CMOS-SRWSN interface uses MCM techniques and a few components fabricated in different technologies for a large spectrum of applications. Furthermore, in terms of project and design, it is easier to provide the supply, when all the system blocks are integrated together in the same microsystem, because the feeding points are reduced and the battery coupling is more effective. Thus, the key of effective wireless interfaces for vehicles relies on a tradeoff between the best baud rates and control features, as it is the case of high-performance embedded systems.

The CMOS-SRWSN interface is used to connect the sensors spanned in the car and to transmit the acquired values to a base station, which stores, processes, and displays the most suitable physical measures, such as the oil level, the water temperature in the cooling system, and the pressures in the tires, besides others. These measurements can be monitored and displayed in the front panel of the car to give information to the driver while the car is rolling in the road. Another way of using these wireless sensor networks is when the car driver wants to see in a personal digital assistant, for example, the oil level of the engine, without the need to move closer to the car. Fig. 1 shows the system architecture using the CMOS-SRWSN interface to mount a wireless sensor network in a car. This interface overcomes the gap brought by the previous network standards for cars; thus, it allows one to have a real network infrastructure in which the sensing subsystem and the information communication and entertainment system (ICE) coexist.

III. Transceiver Design

The United Microelectronics Corporation (UMC) RF 0.18-μm CMOS process was used for the fabrication of a 2.4-GHz RF transceiver. This process has a polysilicon layer and six metal layers, allowing integrated spiral inductors (with a reasonable quality factor), high resistor values (a special layer is available), and a low-power supply of 1.8 V. This allows an even higher on-chip integration, with the

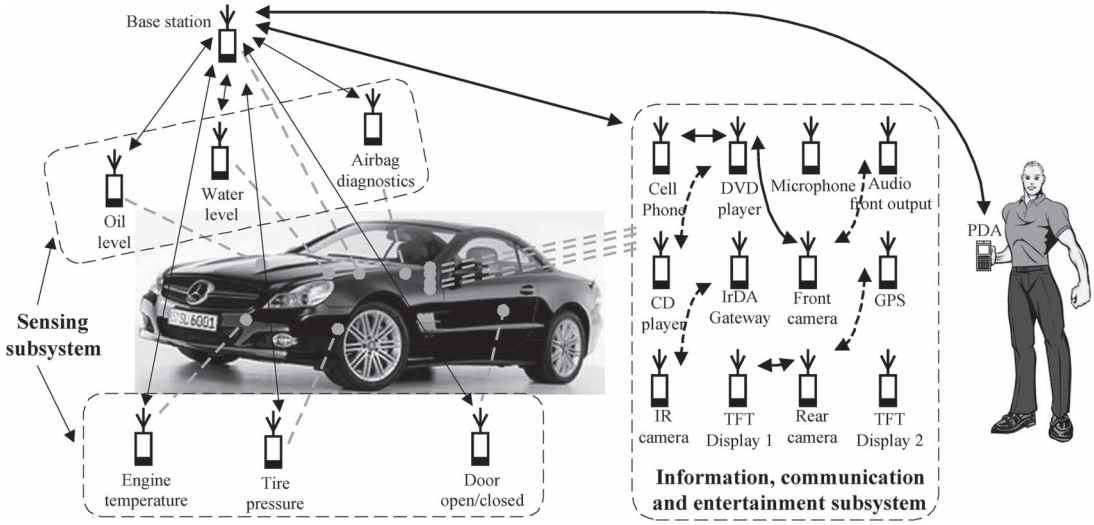

Fig. 1. System architecture using the CMOS-SRWSN.

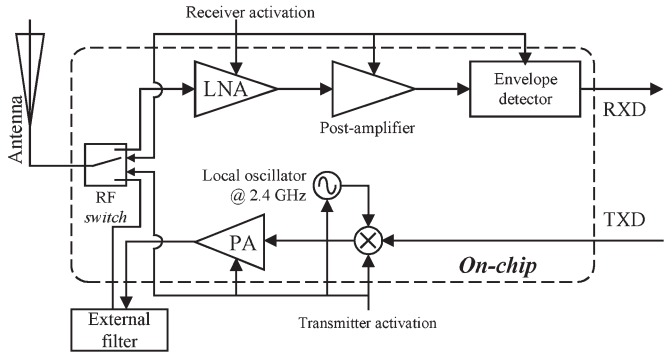

Fig. 2. Block schematic of the transceiver.

additional advantage of better repeatability as well as a lesser pin count.

Without proper design, communication tasks may significantly increase network power consumption because listening and emitting are power-intensive activities [17]. Thus, in order to optimize the power consumption, the RF transceiver design predicts the use of control signals, whose functions can be used to enable and disable all the transceiver subsystems. These signals allow the switching off of the receiver when an RF signal is being transmitted, the switching off of the transmitter when an RF signal is being received, and the transceiver to enter into sleep when RF signals are neither being transmitted nor received. Fig. 2 shows the architecture of the transceiver, which consists of a receiver, a transmitter, and a frequency synthesizer. The receiver adopts a direct demodulation by means of envelope detection.

The power budget of the RF link must be made in order to have, in any noise condition and with the maximum baud rate of 250 kb/s, a bit error probability (BEP) that is less than 10^{-6}. This target quality of service (QoS) is for a maximum transmitted power of $P_T = 0$ dBm ($p_t = 1$ mW) with amplitude shift keying (ASK) modulation. Using an antenna with an output impedance of 50 Ω (at the frequency of 2.4 GHz) and a spectrum analyzer, model *Agilent E4404-B*, several noise measurements were made. It was observed that the noise power never crossed above $N = 10\log_{10}(n) = -104$ dB, where n is the noise power expressed in watts. The previously known noise levels and the QoS of the system are mandatory in order to know the minimum sensitivity of the receiver. Starting with the equation that gives the BEP for ASK with envelope detection [18] $BEP = 1/2\mathrm{e}^{-1/2\gamma}$ $(\gamma \gg 1)$, where γ is the signal-to-noise ratio (SNR) at the receiver (calculated as $\gamma = p_r/n$, where p_r (in watts) and n (in watts) are the signal and noise powers in the receiver site), and in order to have $BEP \leq 10^{-6}$, a minimum SNR in the receiver site of $\gamma \geq 26$ ($\gamma_{\mathrm{dB}} = SNR = 10\log_{10}(\gamma) = 10\log_{10}(p_r/n) = P_R - N = 14$ dB) is necessary. This imposes a minimum signal power $S_{\min}$ (in dBm) in the receiver such that $\gamma_{\mathrm{dB}} = P_R - N \geq S_{\min} - N \geq 14$ dB. Then, the sensitivity of the receiver must be at least $S_{\min} = 14 + N = -90$ dB $\underline{\Delta} - 60$ dBm. From the transmitted power $P_T = 0$ dBm $\underline{\Delta} - 30$ dB and applying the free-space loss equation [19] $\mathrm{PL}_F(d_m) = 20\log_{10}[75/(\pi d_m f_{\mathrm{MHz}})]$, where d_m is the distance (in meters) and f_{MHz} is the frequency (in megahertz), the $SNR = 10\log_{10}(SNR)$ (in decibels) for a 10-m range is such that $\gamma_{\mathrm{dB}} = P_T - \mathrm{PL}_F(d_m = 10\ \mathrm{m}) - N \cong +13.96$ dB. This SNR is very close the required $+14$ dB with a relative error less than 0.29%.

A. Receiver

Fig. 3 shows the receiver's front-end schematic. In a typical receiver, the LNA is the first gain stage in the receiver path; thus, in an LNA, the signal must be amplified as much as possible, with a small SNR decrease. This is achieved with the best noise figure (NF). The LNA is an inductively degenerated common source amplifier [20]. This makes the input impedance at 2.4 GHz equal to 50 Ω, for matching with an antenna switch. A cascading transistor M_2 is used to increase the gain, to better isolate the output from the input, and to reduce the effect of M_1's C_{gs}. The LNA is placed in sleep mode when the current in the polarization stage ceases to flow. The same principle applies to all subsystems of the transceiver. The inductance L_s is implemented with the bonding connection to the external printed circuit board (PCB), which has been calculated to be

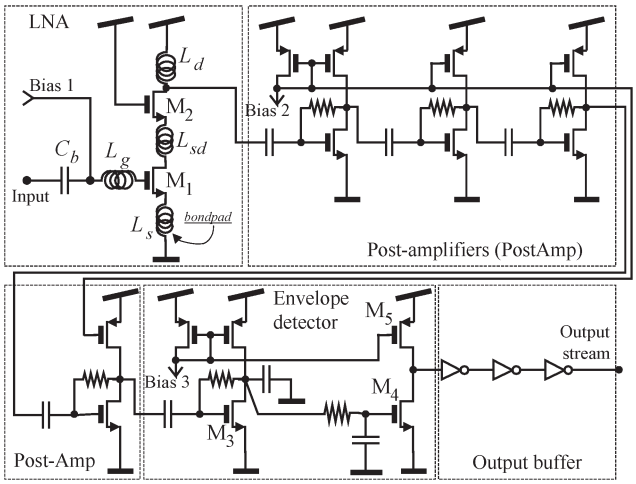

Fig. 3. Full schematic of the receiver.

0.9 nH/mm [21]. The wires used to connect the die to an external PCB, with an RF substrate, has an inductance that adds to the LNA circuit. The use of the inductance $L_{\rm sd}$ helps to reduce these effects.

For this LNA, the input impedance is given by $Z_{\rm in} = sL_g + 1/(sC_{\rm gs}) + L_s[(g_{m1}/C_{\rm gs}) + s]$, and the input matching is made by trimming the L_s and L_g inductances. The matching is achieved when the input impedance is equal to the impedance $Z_{\rm ant}$ of the antenna, where the most common value is 50 Ω. The start-up point in an LNA design is to get the width for the transistor M_1, whose optimal value is $W_{\rm opt} = (6\pi f_c {\rm LC}'_{\rm ox} Z_{\rm in})^{-1}$ (in micrometers), where f_c (in hertz) is the working frequency of the LNA, L (in micrometers) is M_1's length, $C'_{\rm ox}$ (in farad per square meter) is the oxide per area unit capacitance, and finally, $Z_{\rm in}$ is the input impedance of the LNA, which is desired to be purely real and equal to 50 Ω. The oxide per area unit capacitance is $C'_{\rm ox} = \varepsilon_{\rm ox}/T_{\rm ox}$, where $T_{\rm ox}$ (in meters) is the SPICE parameter, which defines the oxide thickness [22]. The parameters $T_{\rm ox} = 4.2 \times 10^{-9}$ m and $\varepsilon_{\rm ox} = 4.1\varepsilon_0 = 4.1 \times 8.85$ aF $\cdot\ \mu{\rm m}^{-1}$ presented in the UMC 0.18-μm RF CMOS process help to obtain the oxide per area unit capacitance $C'_{\rm ox} = 8639.3$ aF $\cdot\ \mu{\rm m}^{-2} = 8.6393$ mF $\cdot\ {\rm m}^{-2}$. Thus, the optimal width that simultaneously minimizes the consumption and the NF of the LNA is equal to $W_{\rm opt} = 284.29$ μm. The UMC foundry offers transistors optimized for RF operation; thus, the choice fell on these devices, due to its low-noise and better isolation properties, compared with the use of mixed-mode transistors. For such transistors, M_1's gate–source capacitance is $C_{\rm gs} = 830$ fF, and its transconductance is $g_{m1} = 20.27$ mS. Finally, the values for each of the inductances are $L_s = 2.01$ nH and $L_g = 3.27$ nH. The most suitable block capacitance at the input of the LNA is $C_b = 10$ pF. The observed current at the drain of the transistor M_1 is 2 mA. This is the minimum achievable limit for the current supply.

In order to avoid mismatching problems related to the passive elements of the circuit, the design must predict, as much as possible, the integration of RF components. This also applies to all dc blocking capacitors. The values of the previous inductances were obtained for a capacitance $C_{\rm gs}$ for a transistor with an arbitrary width $W = W_{\rm opt}$ (in micrometers). The width of RF-optimized transistors cannot be any value; in fact, this value depends on the number of fingers in the MOSFETs. For each MOSFET transistor, the maximum number of fingers are twenty one (21), e.g., the maximum width is limited to 105 μm. This was the first reason for making the width of M_1 equal to 105 μm against the optimal value $W_{\rm opt}$. The second reason deals with the fact of having a small dc block capacitance $C_b = 2$ pF, e.g., it occupies less chip area compared with 10 pF; thus, it is more easy to integrate this capacitor in the same die of the LNA. Under these conditions, the new value for the parasitic gate–source capacitances of the MOSFETs M_1 and M_2 is $C_{\rm gs} = 129.94$ fF. Thus, the internal inductance at the source and the transconductance of the MOSFETs are $L_{\rm s\_int} = 41.2$ pH and $g_{\rm m1} = 21.28$ mS, respectively. These values were calculated for the drain–source voltage $V_{\rm ds} = 1.03$ V and for the bias voltage $V_{\rm gs} = 579$ mV. The gate inductance was further adjusted to the new value $L_g = 21$ nH because it was not possible to achieve a satisfactory gain with the previous value. The inductance $L_{\rm sd}$ helps to increase the gain and to lower the return loss of the LNA. The inductance connected to the drain of M_2 measures $L_d = 4.4$ nH and is tuned to the 2.4-GHz frequency by means of a 1-pF capacitance.

A minimum RF level at the envelope detector is achieved by means of further amplification of the signal at the LNA output. This minimum level defines the receiver's sensitivity. Basically, the idea of the envelope detector is as follows: An increase in the input amplifier implies a decrease in the M_3 gate voltage (this keeps the branch current constant), meaning a decrease in M_4's gate voltage (after filtering), thus decreasing the transistor M_4 current itself. When this current reaches a point that cancels with the transistor M_5 mirror current, the output capacitance starts to discharge, and the output voltage goes high.

This circuit was tested for an input signal modulated in ASK and with an amplitude of 200 mV. It was observed that, when the carrier ceases, the output voltage does not decay immediately from 1.8 V to zero. The most severe situation in terms of receiving jitter is when the data transmission is made with the maximum baud rate of 250 kb/s. In this situation, the observed jitter does not exceeded 20 ns, which corresponds to only 0.005 b.

B. Transmitter

The ASK modulated signal is generated by means of a switched power amplifier. The power amplifier has a cascade of five inverters in order to drive the ASK output signal to the input of the power amplifier. Fig. 4 shows the schematic of the whole transmitter, where one can see the power amplifier, as well as a power select circuit that makes possible the selection of the transmitted power. The network L_1–C_1 is tuned to the carrier frequency, while the emissions outside the 2.4-GHz band are reduced by the network L_2–C_2.

C. Frequency Synthesizer

The phase-locked loop (PLL) has a reference generator circuit with a crystal-based oscillator at 20 MHz, followed by a phase-frequency difference circuit (PFD), a current steering

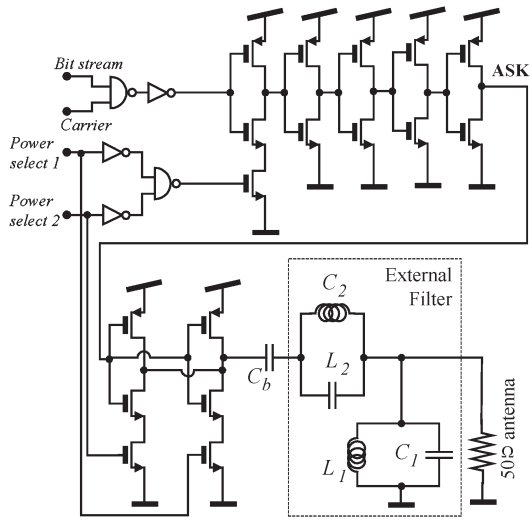

Fig. 4. Schematic of the transmitter.

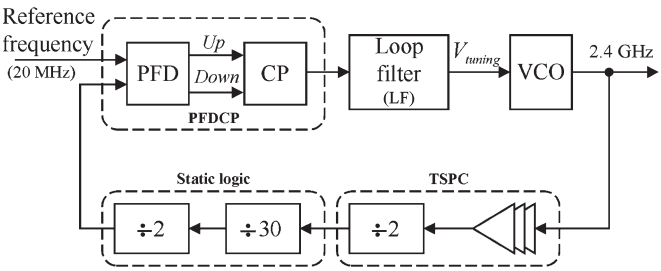

Fig. 5. PLL structure.

charge pump (CP), and a third-order passive filter. The passive section output is connected to the voltage-controlled oscillator (VCO) that generates the desired frequency of 2.4 GHz. This frequency must be divided by 120 and connected to the PFD again, closing the loop (see Fig. 5). The PFD has a linear gain in the range $[-\pi, +\pi]$ and a large constant gain in the ranges $[-2\pi, -\pi]$ and $[+\pi, +2\pi]$ [23]. These PFDs make PLLs faster, compared with those using conventional PFDs.

The CP is of current steering type. This circuit avoids the conventional problem in CPs that limits the opening and closing of current sources; in fact, in spite of being switched, the current is routing from the load to an alternative path and from that path to the load.

A current-starved ring oscillator was used as VCO. Ring oscillators have more phase noise than oscillators. For overcoming this limitation, the bandwidth of the PLL must be high enough to "clean up" the output spectrum around 2.4 GHz.

A third-order passive filter, composed by second- and first-order sections, providing an additional pole is used. The first-order filter reduces spurs caused by the multiples of reference frequency, whose consequence is the increase of the phase noise at the output. The stability is guaranteed by putting this last pole five times above the PLL bandwidth and below the reference. A bandwidth of approximately two times the difference between the maximum and minimum frequencies generated by the VCO was used. The stability in the loop is obtained with a phase margin of $\pi/4$ rad. The division by 120 in the feedback path is done with a cascade constituted by one

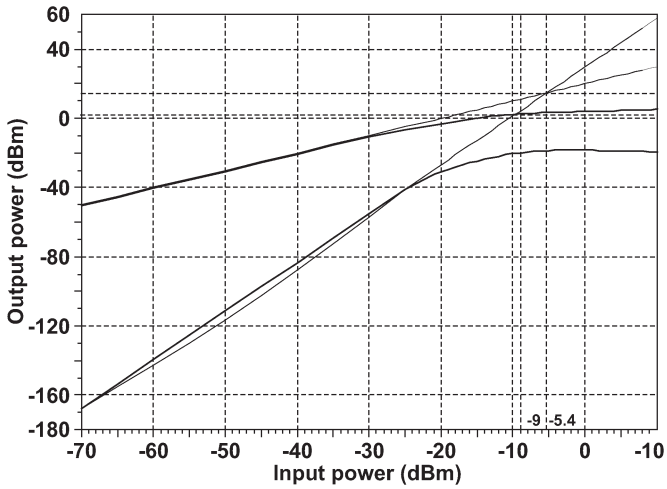

Fig. 6. IP1 and IP3 of the LNA.

half divider implemented with a true single phase clock (TSPC) logic [24], one divider by 30, followed by a toggle flip-flop to ensure a duty cycle of 50% at the PFD input. The TSPC logic was used to overcome the impossibility of implementing the first toggle flip-flop with static logic in this technology. A rail-to-rail input is required for it to work properly. A ratio of 30 was achieved with the use of frequency dividers by 2/3 with modulus control.

D. Antenna Switch

The receiver or transmitter subsystems are connected to the antenna by means of a digitally controlled antenna switch. The isolation between nonconnected ports must be high, keeping the losses between connected ports lowest. For a compact RF front end, the integration of the antenna switch must be in the same die of the transceiver.

IV. Experimental Results

The experimental tests made to the RF CMOS transceiver show a total power consumption of 6.3 mW for the receiver (4 mW for the LNA and 2.3 mW for the envelope detector and the postamplifier) and 11.2 mW for the transmitter. The transmitter delivers a maximum output power of 1.28 mW (very close to the specified 0 dBm) with a power consumption of 11.2 mW. When enabled, the power at the output of the power amplifier can be selected from the following values: 0.22, 1.01, and 1.28 mW. As shown in Fig. 6, for the LNA, a S_{21} of 19.2 dB, an NF of 3 dB, a 1-dB compression point (IP1) of -9 dBm, and a third-order intercept point (IP3) of -5.4 dBm were observed. The LNA has also a stabilization factor of $K = 1.8$ (greater than the unity) that makes this amplifier unconditionally stable.

The CP has a detector constant gain $K_\phi = 175\ \mu\text{A}/2\pi$ rad. The transistor M_2 at the VCO allows one to keep the oscillations when the voltage at the gate of the transistor M_1 falls below its threshold voltage V_{th}. This makes it possible to control the VCO at the full range [0, 1.8 V], providing a frequency range of [2.02, 2.76 GHz] with a tuning constant $K_{\text{VCO}} = 876.6$ MHz/V, calculated in the linear working range

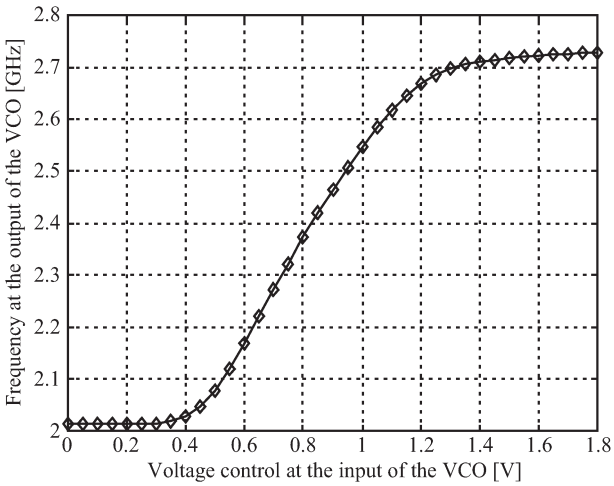

Fig. 7. Measured working characteristic of the VCO.

(see Fig. 7). The judicious selection of the loop filter allows one to have, for this PLL, a minimum time to lock of 1.6 μs, e.g., less than half a bit duration time at a maximum baud rate of 250 kb/s.

Finally, the antenna switch provides a minimum port isolation of 41.5 dB and a maximum insertion loss of 1.3 dB. A commercial antenna of planar type was selected, measuring 6.1 mm $\times$ 3.1 mm $\times$ 1 mm and weighing 0.05 g. This antenna has a maximum return loss of 2.5, a bandwidth of 40 MHz, an efficiency of 55%, and a nominal impedance of 50 Ω at the [2.4, 2.5 GHz] frequency range.

V. CMOS-SRWSN Interface for Automotive Applications

The CMOS-SRWSN interface is composed of a sensor interface that provides protection against electrostatic discharge (ESD). It is also composed of the electronics for processing and control, the memory, an RF transceiver, and a pair of bounding pads to make the connection to an associated antenna. All of these components are integrated in the same microsystem by the use of MCM techniques. The results of the tests made to the ESD protections are documented in [25], and it was proven to be efficient. These ESD protections are of special utility in automotive environments, due to the nature of such environment, which is rich in electromagnetic interferences and high-voltage sparks. Fig. 8 shows the block diagram of the proposed RF microsystem to be used in the plug-and-play modules for application in cars.

The wireless communication is between the base station and the multiple processing elements placed in the car. The main advantage is the fact that the sensors can be positioned where they are necessary. The sensors can also be removed when they are no longer required. The modules must offer the plug-and-play feature in order to mount distributed networks in the car. Moreover, as the acquired data are periodically acquired in all the modules, the latencies of data transmissions are not allowed. The proposed modules use a communication protocol that overcomes these problems [26]. The protocol combines the

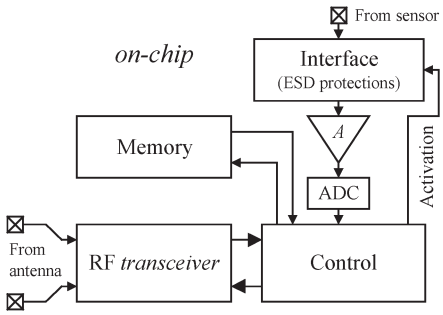

Fig. 8. Block diagram of microsystems for use in cars.

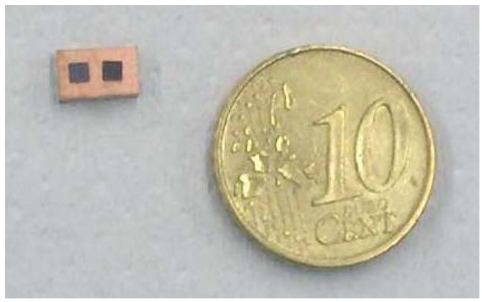

Fig. 9. Module photograph showing the electronics (microchip on the left), the RF transceiver (microchip on the right), and a planar antenna.

distributed and coordination modes, e.g., when a new module is placed, a contention-based time interval is used to make the registration request in the network. A contentionless time interval, constituted by time slots, is granted to the new module if the registration is successfully completed on the network. The maximum number of simultaneous modules is limited to the number of time slots in the contention-free interval. A network coordinator periodically generates a beacon to allow frame synchronization in order to let the different nodes know when they start the time slot for which they were granted access to the medium. The Manchester coding was used in the symbol synchronization for ASK transmission, e.g., for each data bit to be sent, a set of two Manchester symbols are transmitted at twice the bit rate. More precisely, if a "1" or a "0" is to be sent, then the Manchester sequence "10" or "01" is transmitted during the duration of a bit. Moreover, this is particularly useful in the presence of long data sequences of "1s" or "0s." This communication protocol ensures that the conceptual separation between the sensing and the information, communication, and entertainment subsystems is obtained and that their coexistence is achieved. Furthermore, the power-selection feature offered by the RF transmitter makes it possible to include a power-efficient variant in this protocol.

Fig. 9 shows a photograph of a full wireless module, where the processing and control electronics (the microchip on the left) and the RF transceiver (the microchip located on the right) mounted together with an associated antenna are shown. The whole electronics and the associated antenna must be placed very close to the sensors in a car. The use of these plug-and-play modules makes it possible to mount a wireless sensor network in a car.

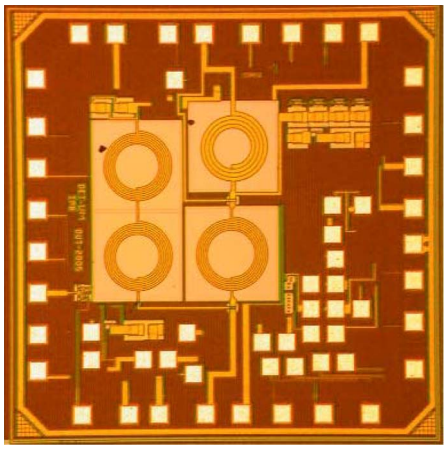

Fig. 10. Die photograph of the RF CMOS transceiver.

TABLE I
COMPARISON OF THE CMOS-SRWSN INTERFACE WITH OTHER EXISTING STANDARDS IN VEHICULAR ENVIRONMENTS

	CMOS-SRWSN	Bluetooth [13]	ZigBee [10]	UWB [2]
Baud-rate [kbps]	250	1000	20-250	20-250
Range [m]	10	1-10	10-100	1-100
Network size	2-60	1 master + 7 slaves	2-65000	256/65536
Network topology	Combined distributed & coordinating	Star	Star, Mesh or Hybrid	Star, Mesh or Hybrid
MAC protocol	Hybrid TDMA & CSMA-CA	TDMA	CSMA-CA & TDMA	CSMA-CA & TDMA
Modulation & coding	ASK & Manchester	GFSK & FHSS	OQPSK & DSSS	DS-UWB
TX power [mW]	<1	1-100	< 1	1 mW/Mbps
Power profile	Application dependent	Days	Years	-
Application focus	Customised sensing & control	Cable replacement	Remote sensing & control	Ranging, location & multimedia

VI. CONCLUSION

A CMOS-SRWSN interface comprising a sensor readout, electronics of processing and control, a memory, an RF transceiver, and a planar antenna has been presented in this paper.

Fig. 10 shows the photograph of the RF transceiver die, which was fabricated in the UMC RF CMOS 0.18-μm process and occupies an area of 1.5×1.5 mm^2. The receiver has a sensitivity of -60 dBm and consumes 6.3 mW from a 1.8-V supply. The transmitter delivers an output power of 0 dBm with a power consumption of 11.2 mW. The CMOS-SRWSN interface can be compared with the other solutions in the Table I [2].

These characteristics fulfill the requirements for short-range communications in using the 2.4-GHz industrial, scientific, and medical bands. The CMOS-SRWSN interfaces are suitable for the fabrication of modules to be deployed as individual nodes of a wireless sensor network and to support the information, communication, and entertainment systems in cars.

REFERENCES

[1] S. Krueger and F. Solzbacher, "Applications in intelligent automobiles," *MSTNEWS—International Newsletter on Microsystems and MEMS*, pp. 6–10, Feb. 2003.

[2] M. Ahmed, C. U. Saraydar, T. ElBatt, J. Yin, T. Talty, and M. Ames, "Intra-vehicular wireless networks," in *Proc. Globecom*, Nov. 2007, pp. 1–9.

[3] J. P. Carmo, P. M. Mendes, C. Couto, and J. H. Correia, "RF microsystems for wireless sensors networks," in *Proc. DTIS*, Cairo, Egypt, Apr. 2009, pp. 52–57.

[4] T. ElBatt, C. Saraydar, M. Ames, and T. Talty, "Potential for intra-vehicle wireless automotive sensor networks," in *Proc. Sarnoff Symp.*, Mar. 2006, pp. 1–4.

[5] H.-M. Tsai, W. Viriyasitavat, O. K. Tonguz, C. Saraydar, T. Talty, and A. Macdonald, "Feasibility of in-car wireless sensor networks: A statistical evaluation," in *Proc. 4th Annu. IEEE SECON*, Jun. 1007, pp. 101–111.

[6] J. Li and T. Talty, "Channel characterization for ultra-wideband intra-vehicle sensor networks," in *Proc. IEEE Mil. Commun. Conf.*, Washington, DC, Oct. 2006, pp. 1–4.

[7] W. Niu, J. Li, and T. Talty, "Ultra-wideband channel modeling for in-travehicle environment," *EURASIP J. Wireless Commun. Netw.*, vol. 2009, p. 806 209, 2009, 12 pages, DOI:10.1155/2009/806209.

[8] W. Niu, J. Li, S. Liu, and T. Talty, "Intra-vehicle ultra-wideband communication testbed," in *Proc. IEEE Globecom*, Nov. 2008, pp. 1–5.

[9] E. Peterson, *An Investigation Into Intra-Vehicle Sensor Networks*, 2006.

[10] H.-M. Tsai, O. K. Tonguz, C. Saraydar, T. Talty, M. Ames, and A. Macdonald, "ZigBee-based intra-car wireless sensor networks: A case study," *IEEE Wireless Commun.*, vol. 14, no. 6, pp. 67–77, Dec. 2007.

[11] J. A. Flint, A. R. Ruddle, and A. E. May, "Coupling between Bluetooth modules inside a passenger car," in *Proc. 12th IEEE ICAP*, Apr. 2003, pp. 397–400.

[12] A. Schoof, T. Stadtler, and J. L. ter Hasborg, "Simulation and measurements of the propagation of Bluetooth signals in automobiles," in *Proc. IEEE Int. Symp. Electromagn. Compat.*, May 2003, pp. 1297–1300.

[13] G. Leon and D. Heffernan, "Vehicles without wires," *Comput. Control Eng. J.*, vol. 12, no. 5, pp. 205–211, Oct. 2001.

[14] P. Andreas and W. Zimdahl, "The driver information of the Volkswagen research car auto 2000," *IEEE Trans. Ind. Electron.*, vol. IE-30, no. 2, pp. 132–137, May 1983.

[15] F. Gil-Castineira, F. J. Gonzalez-Castano, and L. Franck, "Extending vehicular CAN fieldbuses with delay-tolerant networks," *IEEE Trans. Ind. Electron.*, vol. 55, no. 9, pp. 3307–3314, Sep. 2008.

[16] J. Hill, R. Szewczyk, A. Woo, S. Hollar, D. E. Culler, and K. S. J. Pister, "System architecture directions for networked sensors," in *Proc. Architectural Support Program. Languages Operating Syst.*, 2000, pp. 93–104.

[17] C. C. Enz, A. El-Hoiydi, J. D. Decotignie, and V. Peiris, "WiseNET: An ultra low-power wireless sensor network solution," *Computer*, vol. 37, no. 8, pp. 62–70, Aug. 2004.

[18] A. B. Carlson, P. B. Crilly, and J. C. Rutledge, *Communication Systems—An Introduction to Signals and Noise in Electrical Communications*, 4th ed. New York: McGraw-Hill, 2001.

[19] J. Parsons, *The Mobile Radio Propagation Channel*, 2nd ed. Hoboken, NJ: Wiley, 2000.

[20] A. Abidi, "CMOS wireless transceivers: The new wave," *IEEE Commun. Mag.*, vol. 37, no. 8, pp. 119–124, Aug. 1999.

[21] F. Alimenti, P. Mezzanotte, L. Roselli, and R. Sorrentino, "Modeling and characterization of the bonding-wire interconnection," *IEEE Trans. Microw. Tech.*, vol. 49, no. 1, pp. 142–150, Jan. 2001.

[22] *UMC Spec. No. G-04-LOGIC18-1P6M-INTERCAP, Ver. 1.7, Phase 1 UMC 0.18 μm 1P6M Logic Process Interconnect Capacitance Model*, Aug. 2001.

[23] B. Kim and L. Kim, "A 250-MHz–2-GHz wide-range delay-locked loop," *IEEE J. Solid-State Circuits*, vol. 40, no. 6, pp. 1310–1321, Jun. 2005.

[24] S. Pellerano, S. Levantino, C. Samori, and A. L. Lacaita, "A 13.5 mW 5-GHz frequency synthesizer with dynamic logic frequency divider," *IEEE J. Solid-State Circuits*, vol. 39, no. 2, pp. 378–383, Feb. 2004.

[25] J. P. Carmo, P. M. Mendes, C. Couto, and J. H. Correia, "Effects of the ESD protections in the behavior of a 2.4 GHz RF transceiver: Problems and solutions," in *Proc. Int. Symp. Ind. Electron.*, Cambridge, U.K., Jun. 2008, pp. 935–938.

[26] J. Afonso, H. R. Silva, L. A. Rocha, and J. H. Correia, "MAC protocol for low-power real-time wireless sensing and actuation," in *Proc. 13th IEEE Int. Conf. Electron., Circuits Syst.*, Nice, France, pp. 1248–1251.

João Paulo Carmo (S'02–M'08) was born in Maia, Portugal, in 1970. He received the B.S. and M.Sc. degrees in electrical engineering from the University of Porto, Porto, Portugal, in 1993 and 2002, respectively, and the Ph.D. degree in industrial electronics from the University of Minho, Guimarães, Portugal, in 2007. His Ph.D. thesis was on RF transceivers for integration in microsystems to be used in wireless-sensor-network applications.

Since 2008, he has been an Assistant Researcher in the Algoritmi Center, Department of Industrial Electronics, University of Minho. He is involved in research on micro-/nanofabrication technologies for mixed-mode/RF systems, solid-state integrated sensors, microactuators, and micro-/nanodevices for use in wireless and biomedical applications.

Dr. Carmo is a member of the IEEE Industrial Electronics Society.

Paulo Mateus Mendes (M'05) received the B.S. degree and the M.Sc. degree in electrical engineering from the University of Coimbra, Coimbra, Portugal, in 1995 and 1999, respectively, and the Ph.D. degree in industrial electronics from the University of Minho, Guimarães, Portugal, in 2005.

Since 2006, he has been an Assistant Professor at the University of Minho, where he is a Researcher in the Algoritmi Center. He has been involved in several projects related to projection, fabrication, and characterization of microantennas for wireless microsystems.

Dr. Mendes is a member of the European Microwave Association, the IEEE Antennas and Propagation Society, and the IEEE Engineering in Medicine and Biology Society.

Carlos Couto (SM'03) received the B.S. degree in electrical engineering from the University of Lourenço Marques, Lourenço Marques, Mozambique, in 1972, and the M.Sc. and Ph.D. degrees in power electronics from the University of Manchester Institute of Science and Technology, Manchester, U.K., in 1979 and 1981, respectively.

In 1976, he joined the University of Minho, Guimarães, Portugal, where, since 1995, he has been a Full Professor in the Department of Industrial Electronics. His research interests are microsystems, instrumentation, and power electronics.

Prof. Couto is a member of the IEEE Industrial Electronics Society.

José Higino Correia (S'96–M'00) received the B.S. degree in physical engineering from the University of Coimbra, Coimbra, Portugal, in 1990, and the Ph.D. degree from the Laboratory for Electronic Instrumentation, Delft University of Technology, Delft, The Netherlands, in 1999, working in the field of microsystems for optical spectral analysis.

Currently, he is a Full Professor in the Department of Industrial Electronics, University of Minho, Guimarães, Portugal. His professional interests are micromachining and microfabrication technology for mixed-mode systems, solid-state integrated sensors, microactuators, and microsystems.

Prof. Correia was the General Chairman of Eurosensors 2003 and Micromechanics and Microengineering Europe 2007, held in Guimarães. He is a member of the IEEE Industrial Electronics Society.